Breakdown of phase rigidity and variations of the Fano effect in closed Aharonov-Bohm interferometers

Amnon Aharony,[1,2,3] Ora Entin-Wohlman,[1,2,3] Tomohiro Otsuka,[1] Shingo Katsumoto,[1,*] Hisashi Aikawa,[1,†] and Kensuke Kobayashi[1,‡]

[1]*Institute for Solid State Physics, University of Tokyo, 5-1-5 Kashiwanoha, Chiba 277-8581, Japan*

[2]*School of Physics and Astronomy, Raymond and Beverly Sackler Faculty of Exact Sciences, Tel Aviv University, Tel Aviv 69978, Israel*

[3]*Physics Department, Ben Gurion University, Beer Sheva 84105, Israel*

(Received 16 December 2005; revised manuscript received 16 February 2006; published 30 May 2006)

Although the conductance of a closed Aharonov-Bohm interferometer, with a quantum dot on one branch, obeys the Onsager symmetry under magnetic field reversal, it needs not be a periodic function of this field: The conductance maxima move with both the field and the gate voltage on the dot, in an apparent breakdown of "phase rigidity." These experimental findings are explained theoretically as resulting from multiple electronic paths around the interferometer ring. Data containing several Coulomb blockade peaks, whose shapes change with the magnetic flux, are fitted to a simple model, in which each resonant level on the dot couples to a different path around the ring.

DOI: 10.1103/PhysRevB.73.195329 PACS number(s): 73.21.La, 72.15.Qm, 73.23.Hk, 85.35.−p

I. INTRODUCTION

The mesoscopic Aharonov-Bohm interferometer (ABI) has been used widely in attempts to measure both the magnitude and the phase of the quantum transmission amplitude for an electron traversing a quantum dot (QD). Many of these experiments have been done on the *closed* ABI, where the QD is placed on one of the two paths which surround an area which is penetrated by a magnetic flux Φ, and the two paths are connected to two reservoirs via only two terminals.[1,2] In some experiments, the states on the whole path replace the QD.[3] Unlike for the multi-terminal *open* ABI, for small fluxes the conductance of the closed interferometer turned out to be an *even and periodic function of the Aharonov-Bohm (AB) phase* $\phi=\Phi/\Phi_0$, with $\Phi_0=\hbar c/e$ and with the period $\Delta\phi=2\pi$. Away from resonances of the transmission, and for relatively small magnetic fields, the conductance of the "ideal" closed ABI could be fitted to the simple (two-slit-like) formula $G=A+B\cos\phi$ and, therefore, its maxima (and minima) remained fixed at integer multiples of π, independent of the gate voltage on the QD (which only affected the values of A and B). This phenomenon, called "phase rigidity," has been accepted as a landmark of the closed ABI.[4,5] Closer to a resonance, G becomes a more complicated function of ϕ, which contains higher harmonics in the flux, but continues to depend only on powers of $\cos\phi$ (and not of $\sin\phi$). Indeed, the symmetry $G(\phi)=G(-\phi)$ is now well understood, due to the Onsager relations.[6] The periodicity of G with ϕ, and the resulting phase rigidity, have also been reproduced theoretically, in models which describe both the paths around the ABI ring and the leads to the reservoirs as being one-dimensional (1D).[7,8] However, although phase rigidity obeys the Onsager symmetry, this rigidity does not really *follow* from this symmetry. In fact, many of the measurements at higher fluxes break phase rigidity.

The breakdown of phase rigidity in experiments on closed ABI's shows up as deviations from the simple pure oscillation $G=A+B\cos\phi$, even far away from resonances. Such deviations already appeared in the pioneering work of Webb *et al.*,[9] which demonstrated the AB oscillations in normal metal rings. In these experiments (and in practically all the other experiments mentioned above), the AB oscillations appear on top of a background, whose slow variation with the magnetic flux has been described as an *aperiodic fluctuation*, due to the penetration of the magnetic field into conducting parts of the ABI ring. Indeed, numerical simulations have shown that such fluctuations do result from the fluxes which penetrate small areas within the finite width of the ring, whose properties fluctuate randomly.[10,11] As noted by Imry,[12] such fluctuations can be observed only at high fluxes, $\Phi \gg \Phi_0/x$, where x is the ratio of the area of the conducting ring to the area of the hole inside it. As Stone and Imry[11] note, this background may also contain beats. However, we are not aware of a detailed theoretical analysis of such beats, or of any other *periodic* aspect of the deviations from a simple Aharonov-Bohm oscillation.

In the first part of this paper we concentrate on two aspects of the breakdown of phase rigidity. First, the "beats." Figure 2 of Ref. 9 already showed two main peaks in the power spectrum of the flux-dependent conductance: One at the Aharonov-Bohm period and the other at a much smaller period (higher field). Ignoring the aperiodic fluctuations, both periods are clearly visible in the flux dependence of the conductance. The ratio of the two periods is presumably related to the ratio between the areas of the ring and of the hole, x. Similar "beats" show up in practically all the experiments on closed ABI's.[3] The second aspect concerns the location of the conductance maxima and the related phase shift. Figure 4 Ref. 2 shows a contour plot of the conductance versus the gate voltage and the magnetic field. In its restricted sense, phase rigidity implies that (except close to resonances) the maxima should be at fixed fields, namely on lines parallel to the gate voltage axis. However, in the data (taken at relatively high fields) these lines have a nonzero slope relative to that axis. Similar slopes show up in many

similar experimental plots (see, e.g., Fig. 4 in Ref. 13, or Fig. 4 of Ref. 14). A slow change of the location of the maxima with increasing magnetic fields is visible even in the original papers by Yacoby *et al.*[1,4] Analysis of the data within a finite narrow window of fields (away from zero) would thus be described by $G \sim \tilde{A} + \tilde{B}\cos(\phi + \delta)$, with a nonzero phase shift δ, which depends on both the flux and the gate voltage, apparently contradicting phase rigidity. (This behavior holds only at large fields; as the field goes to zero, δ also vanishes, in accord with the Onsager requirement.) All of these papers also exhibit a slow variation of the Aharonov-Bohm oscillation amplitude $\tilde{B}$ with increasing field, which is related to the "beats." Below we present some additional experimental data, and give a theoretical discussion of these observations. In particular, we propose a simple theoretical model which captures all the observed phenomena.

The second part of this paper concerns the Fano shape of the Coulomb blockade resonances. In the Coulomb blockade regime, the QD exhibits a sequence of resonances as function of the gate voltage, whenever another electron is added to its bound states. The interference between these states and the continuum of the electrons in the leads then results in the Fano effect,[15,16] which modifies the shape of these resonances. These resonances are further modified once the QD is placed in the ABI.[2] In the experimental papers,[2] each resonance has been fitted to the "standard" Fano asymmetric Breit-Wigner form, $G \propto |e+q|^2/(e^2+1)$, where e is the normalized distance of the gate voltage from its resonance value and q is the so-called "Fano asymmetry parameter," which can become complex at nonzero magnetic fluxes, when time-reversal symmetry is broken. Below we show that *all* the asymmetric resonances can be described by a *single* unified expression for the transmission amplitude, and present fits to the data which demonstrate the utility of this representation for many resonances.[17]

Section II presents some new data, taken from the same mesoscopic closed ABI described in Ref. 2. Section III then proceeds to describe a simple theory, which takes account of the finite width of the ring. Finally, Sec. IV uses this theory to fit experimental data from the ABI.

II. EXPERIMENTAL DATA

For a quantitative discussion of the points listed above, we start by presenting some new data, taken from the same sample described in Refs. 2. As explained there, the closed ring-shaped ABI, shown in Fig. 1, was fabricated by wet etching the 2DEG at an AlGaAs/GaAs heterostructure. Au/Ti metallic gates define the QD and control the gate voltages on the QD (sitting on the lower branch of the ring) and on the reference (upper) branch. The sample was cooled by a dilution refrigerator, the base temperature of which was 30 mK though the electron temperature measured from the line shape of the Coulomb oscillation was around 100 mK.

All our data are found to be symmetric under $\phi \to -\phi$, in agreement with the Onsager relations. In order to investigate the nature of electronic paths in the ring geometry, we first connected all the gates to ground. The sample was hence a simple ring without a dot at this stage. Figure 2 shows a typical flux dependence of the conductance through the ABI, for these grounding conditions. The data clearly show the Aharonov-Bohm oscillations, with a small period as demonstrated in the insets. In addition, apart from some aperiodic fluctuations, the data exhibit oscillations on a larger scale. To quantify these oscillations, Fig. 3 shows the fast Fourier transform (FFT) of these data. The top graph shows the FFT of all the data. Interestingly, the results between ~ 250 and $\sim 280\ \mathrm{T}^{-1}$ seem to contain several separable peaks. The top graph also shows arrows for the Aharonov-Bohm periods associated with the contours A, B, and C in Fig. 1, indicating that all the frequencies in this range can be associated with electron paths which surround the ring between contours A and C. The inset in the top frame shows the same FFT on a semi-logarithmic scale. It is interesting to note that the data contain many higher harmonics, roughly at integer multiples of the first one. The graph in the middle shows fits to these high frequency data with four and with eight Lorentzians, confirming the impression that the fast oscillations are dominated by only a few electron paths. The decomposed peaks are still much broader than the width corresponding to the field range of the whole measurement. This large width probably comes from a bounded range of the field in which a looped path has a larger amplitude in the transmission coef-

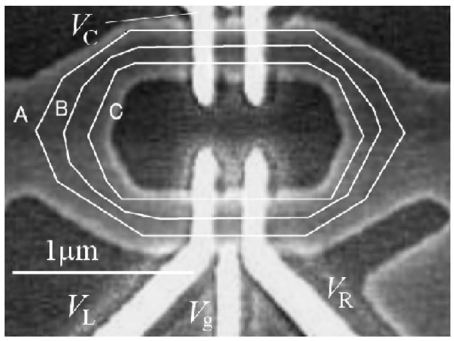

FIG. 1. Scanning electron micrograph of the ABI. White regions are the Au/Ti gates and the corresponding voltages V_L, V_g, V_R, V_C are indicated. The contours A, B, and C indicate possible paths of the electrons.

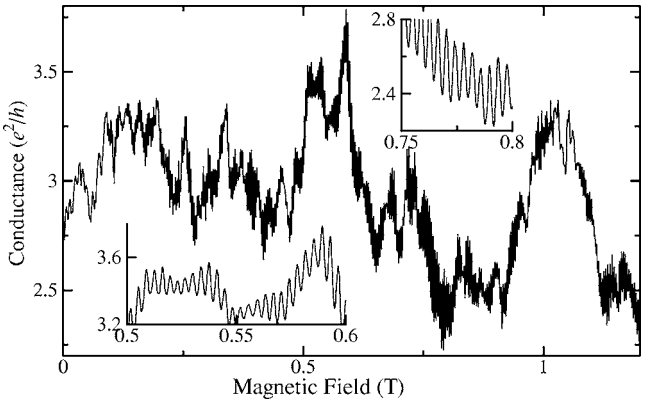

FIG. 2. The conductance of the ABI, with all the gates at zero voltage. The insets are blowups in two different regions of magnetic field.

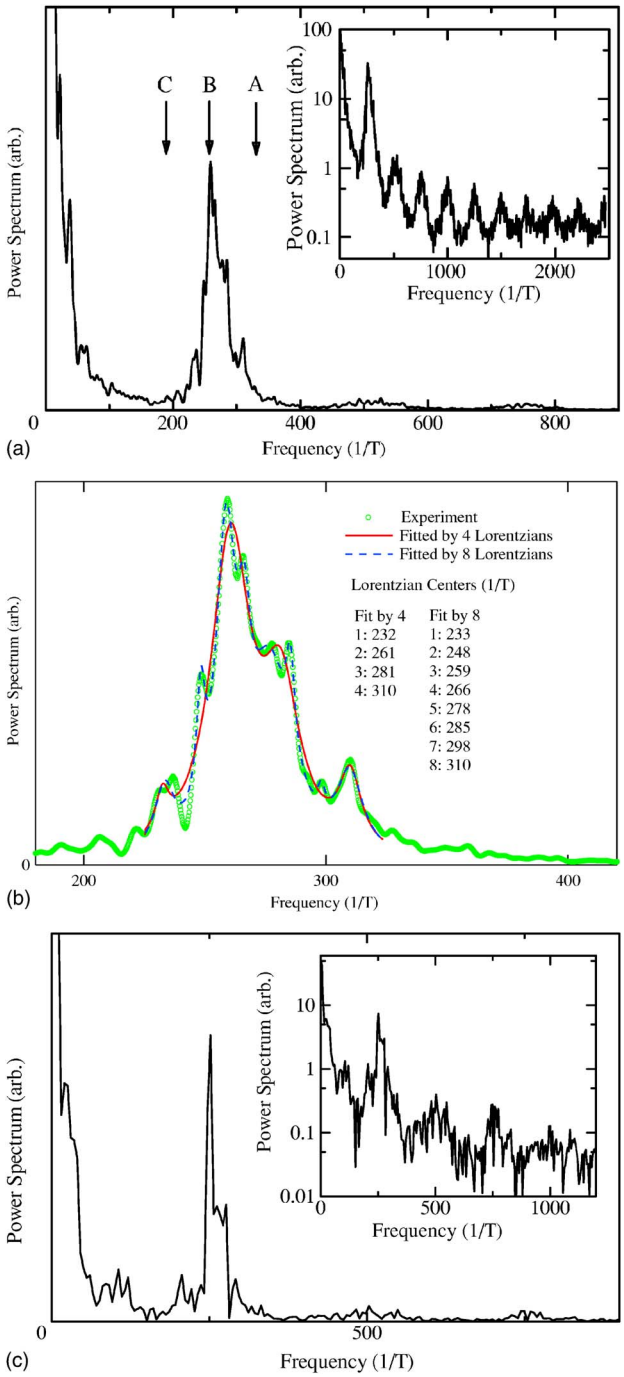

FIG. 3. (Color online) Fourier power spectrum of the data in Fig. 2 (see text). (a) FFT result for the entire field region in Fig. 2. A–C are the frequencies, which correspond to the areas indicated by the contours A–C in Fig. 1. The inset is a log-plot of the same data, enhancing the higher harmonics. (b) Results of the fitting to the main peak in (a) by 4 Lorentzians (solid line) and by 8 Lorentzians (broken line). (c) Result of the same analysis as in (a) for the field region from 0.8 to 1 T.

ficient. Such a slow modulation of amplitude by magnetic field can be caused by, e.g., variation of the boundary scattering probability. The lower graph in Fig. 3 shows the FFT of the data with fields between 0.8 and 1 T. Interestingly, these data exhibit even fewer peaks, implying that these restricted data can be described by "beats" of a few neighboring frequencies. This supports the above interpretation.

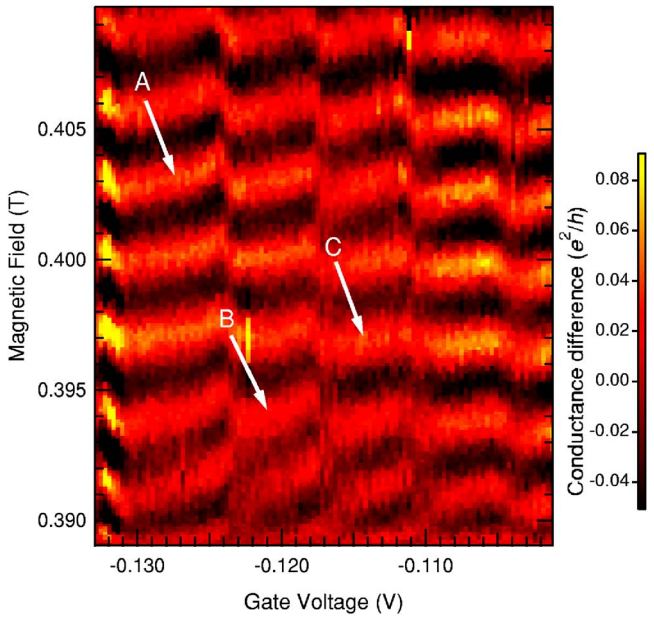

FIG. 4. (Color online) False color image plots of the conductance, versus gate voltage V_g and magnetic field. See the text for other voltages. The linear baseline from 5.3 to 5.7 in (e^2/h) was subtracted.

We have then formed a quantum dot in the lower branch, by applying the gate voltages −0.255 V, −0.215 V for V_L, V_R in Fig. 1, respectively. We also reduced the conductance of the upper (reference) arm, with V_C=−0.26 V. Figure 4 is an image plot of the conductance as function of the gate voltage V_g and the magnetic field. The slowly varying background conductance, which is almost linear in this region from 5.3 to 5.7 in conductance quantum units (e^2/h), was subtracted. Figure 4 clearly demonstrates the breakdown of phase rigidity. Although a similar plot was presented in Ref. 2, the present figure emphasizes several features which we wish to discuss.

In Fig. 4, each resonance is characterized by a narrow region (parallel to the field axis) through which the maxima (red or bright) and minima (black or dark) interchange places. In the ideal 1D model, between resonances the maxima remain fixed at integer multiples of the flux unit, as follows from phase rigidity. In addition, maxima and minima can suddenly interchange between resonances, in a "phase lapse" which is attributed to a Fano vanishing of the conductance. In contrast, the maxima in Fig. 4 never stay on lines parallel to the gate voltage axis. Instead, they move continuously towards larger fields, indicating a nonzero phase shift δ. The variation of the maxima can be characterized by three typical forms, indicated by white arrows: In form A, the maximum moves almost linearly with the gate voltage, so that ϕ changes by π, returning to the value it had before the previous resonance. In form B, one observes a fast change in the location of the maximum, about half way between the resonances. Although reminiscent of the Fano jump by π, this change has a finite width and seems continuous. Finally, in form C the maximum moves by π over the resonance, but

very soon it moves quickly back to its location before the resonance, so that the line of this maximum remains almost parallel to the gate voltage axis for a range of gate voltages.

More experimental data are presented below, in Sec. IV.

III. THEORY

As stated, most of the existing theoretical descriptions of the ABI use models in which all the links are 1D. This means that the ABI "ring" surrounds a well defined unique area, which is penetrated by a *single valued* magnetic flux Φ. It is this uniqueness that then results in the periodicity of G with ϕ, resulting with phase rigidity. To explain the deviation of our (and practically everyone else's) data from this periodicity, we note that the real rings are *never* 1D (see Fig. 1).[9] Due to the finite width of the ABI ring, electrons which move on different paths within the ring surround different areas, and therefore different magnetic fluxes.[9–12] We demonstrate the implications of these different fluxes by a simple tight-binding model, which generalizes models used earlier to describe the ABI in the Coulomb blockade regime.[7,8] Our model is a simplified version of that discussed in Refs. 10 and 11: Instead of the aperiodic random fluctuations, we emphasize the *periodic* influence of the flux through the conducting ring.

One basic difference between our device and that of Webb *et al.*[9] is that our ring is semiconducting, while theirs was metallic. In a semiconductor, we expect the electron to have much fewer possible paths for traversing the ring. This point of view is supported by our discussion of Fig. 3, which shows that the data are dominated by a small number of frequencies. In view of this, our model assumes that each resonance on the quantum dot couples strongly only to a single wave function on the ring, and that each such wave function can be associated with a distinct area and, therefore, with a distinct magnetic flux. Since our theoretical discussion aims to capture the main physical phenomena observed in the experiments, we construct the *simplest* possible theoretical model which reproduces these phenomena. Surprisingly, this model turns out to also give a good *qualitative* fit to our data. Below we comment on why various possible generalizations are not expected to have strong effects on these fits.

In our model, shown in Fig. 5, the QD has N equidistant resonances, at effective energies $E_D(n)=\epsilon_d+(n-1)U$, $n=1,2,\ldots,N$, where ϵ_d is controlled by the gate voltage. (Here, U represents the Coulomb repulsion, within a Hartree approximation, and n represents the nth Coulomb blockade resonance.[8]) Each resonant level is connected to the left and right terminals (L and R) via separate single paths, which may surround different areas. Using gauge invariance, we include the possibly different magnetic fluxes associated with each resonant level in the respective hopping matrix elements, $J_\ell(n)=J_\ell^0(n)e^{i\phi(n)}$ and real $J_\ell^0(n)$ and $J_r(n)$.[18] The phase $\phi(n)$ is associated with the area surrounded by the wave function which couples to the nth resonance. For simplicity, the "reference" site on the lower path of the ABI ring has only one state, with energy E_{ref}, which couples to the sites L and R via real hopping matrix elements j_ℓ and j_r. As we show below, the interference between these different paths gives a conductance which is an even function of the magnetic field (all the $\phi(n)$'s are of course proportional to this field), but has a more complex field-dependence at high fields—similar to the experimental data.

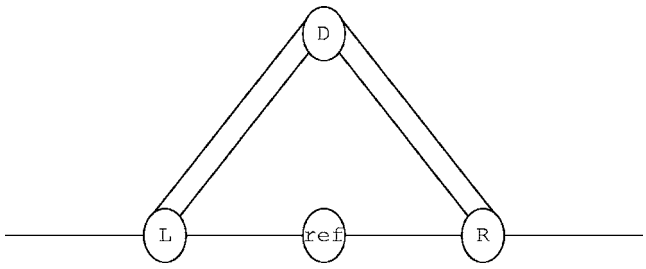

FIG. 5. The model for the ABI: all the tight-binding bonds on the external 1D leads have the same real hopping energy $-J$. L and R connect to each other indirectly, via $(N+1)$ branches (here we show $N=2$): One connects to the reference site, via real hopping coefficients j_ℓ and j_r, while each of the other N connect from L and from R to the quantum dot (D), via hopping coefficients $J_\ell(n)=J_\ell^0(n)e^{i\phi(n)}$ and a real $J_r(n)$.

We next solve the model shown in Fig. 5. The bonds on the semi-infinite external 1D leads have hopping matrix elements $-J$ (below we measure all energies in units of J). For an electron with wave number k and energy $\epsilon=-2J\cos ka$ (a is the lattice constant on the leads), we write the wave functions on the left and right leads as $u(e^{ikna}+re^{-ikna})$ and ute^{ikna} (below we present results in the center of the band, $ka=\pi/2$), and then solve the $N+5$ linear equations in the N wave amplitudes at D, those at L, R and "ref" and in t and r. The resulting transmission amplitude is[19]

$$t=\frac{S_{\ell r}2i\sin ka}{(S_{\ell\ell}+e^{-ika})(S_{rr}+e^{-ika})-|S_{\ell r}|^2}, \tag{1}$$

where

$$S_{xy}=\sum_n \frac{J_x(n)J_y(n)^*}{J[\epsilon-E_D(n)]}+\frac{j_xj_y}{J(\epsilon-E_{ref})} \tag{2}$$

(x,y stand for ℓ,r). Using the Landauer formula,[20] we thus obtain the zero-temperature conductance,

$$\frac{G}{G_0}=T=\frac{4\sin^2 ka|S_{\ell r}|^2}{\left||S_{\ell r}|^2-(S_{\ell\ell}+e^{-ika})(S_{rr}+e^{-ika})\right|^2}, \tag{3}$$

where $G_0=2e^2/h$ is the basic conductance unit and $T\equiv|t|^2$ is the transmission.

It is interesting to note that the transmission T depends on the magnetic field only via the combination

$$\begin{aligned}|S_{\ell r}|^2=&\frac{j_\ell^2j_r^2}{J^2(\epsilon-E_{ref})^2}\\&+\sum_{nn'}\frac{J_\ell^0(n)J_\ell^0(n')J_r(n)J_r(n')}{J^2[\epsilon-E_D(n)][\epsilon-E_D(n')]}\cos[\phi(n)-\phi(n')]\\&+\frac{2j_\ell j_r}{J(\epsilon-E_{ref})}\sum_n\frac{J_\ell^0(n)J_r(n)}{J[\epsilon-E_D(n)]}\cos\phi(n).\end{aligned} \tag{4}$$

Indeed, away from a resonance one has $|S_{xy}|\ll 1$, the field

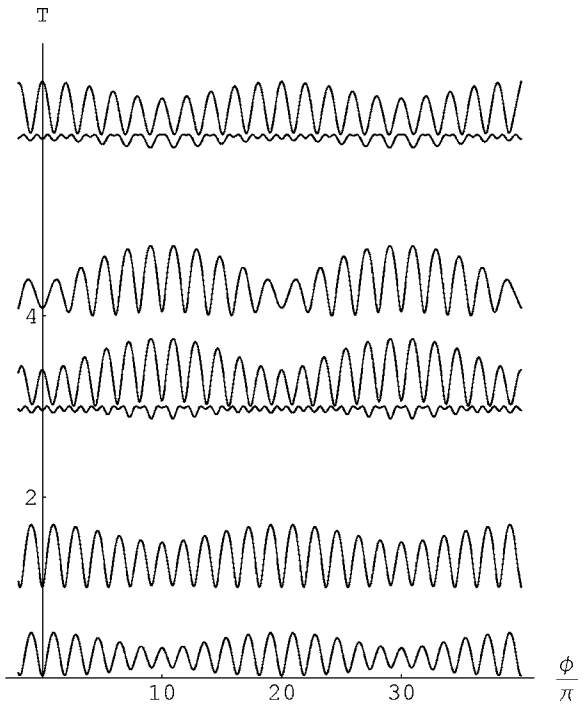

FIG. 6. Transmission through the closed ABI of Fig. 5, vs ϕ, at $\epsilon_d=-5.1, -4, 1, \ldots, 0.9$ for the parameters given in the text. Graphs are shifted up by 1 as ϵ_d increases by 1.

dependence of G in Eq. (3) is dominated by the numerator there, and the maxima (or minima) coincide with those of $|S_{\ell r}|^2$. For $N=2$, this has the form

$$|S_{\ell r}|^2 = A + B_1 \cos\phi(1) + B_2 \cos\phi(2) + C\cos[\phi(1) - \phi(2)]. \tag{5}$$

Since both $\phi(1)$ and $\phi(2)$ correspond to paths through the "upper" branch of the ABI, it is reasonable to expect that these two fluxes are quite close to each other. Assuming a ratio $(1+x)$ between the areas surrounded by the two paths, we denote $\phi(1)=\phi$ and $\phi(2)=(1+x)\phi$, and then Eq. (5) has the form

$$|S_{\ell r}|^2 = A + [B_1 + B_2\cos(x\phi)]\cos\phi - B_2\sin(x\phi)\sin\phi + C\cos(x\phi) \equiv \widetilde{A} + \widetilde{B}\cos(\phi+\delta), \tag{6}$$

with

$$\tan\delta = B_2\sin(x\phi)/[B_1 + B_2\cos(x\phi)],$$

$$\widetilde{B} = \sqrt{B_1^2 + B_2^2 + 2B_1B_2\cos(x\phi)},$$

$$\widetilde{A} = A + C\cos(x\phi). \tag{7}$$

For $|x| \ll 1$, the parameters $\widetilde{A}$, $\widetilde{B}$, and δ vary slowly with ϕ and, therefore, within a limited window of magnetic fields the data look like in the two-slit open ABI, with a phase shift δ which varies with ϕ and with the gate voltage, represented by ϵ_d. On larger field ranges, Eq. (6) exhibits beats, similar to those observed experimentally. Note that the parameters in Eq. (7) may change quite significantly as ϕ changes from zero to π/x. Needless to say, the expression in Eq. (4) and, therefore, also G, is symmetric under field reversal $[\phi(n) \to -\phi(n)$ for all $n]$, as expected from the Onsager relations.

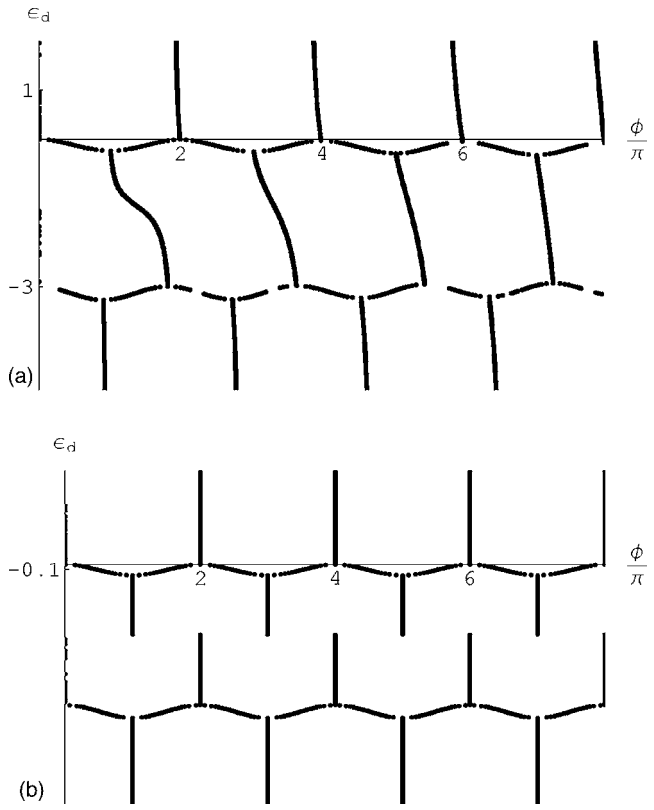

FIG. 7. The location of the maxima of T in the $\phi/\pi - \epsilon_d$ plane. Top: $x=0.1$. Bottom: $x=0$.

When $x=0$, one has $\delta=0$ and $\widetilde{A}$, $\widetilde{B}$ remain constant, as for the simple 1D model. In that limit, the maxima between resonances remain fixed, with possible jumps by π when (B_1+B_2) changes sign as function of the gate voltage ϵ_d.

The above simple results change close to a resonance. To demonstrate the full behavior of the conductance, we present an example with $N=2$, with the parameters $ka=\pi/2$, $j_\ell=j_r=J_\ell^0(n)=J_r(n)=0.5J$, $E_{ref}=J$, $U=3J$, and $x=0.1$. Figure 6 shows the calculated transmission, Eq. (3), for several values of the gate voltage ϵ_d. In addition to seeing the beats away from resonances, we note the asymmetric beats closer to resonances. We also note the gradual shifts in the maxima. These shifts are highlighted in Fig. 7 (top), which shows only the locations of the maxima. This figure contrasts the behavior of the maxima between the ideal 1D case, with $x=0$ (bottom) and the case described above, $x=0.1$ (top). Note particularly the qualitative flux dependence of the maxima locations for gate voltages around $\epsilon_d \sim -1.5$, i.e., midway between the two resonances: for $x=0$ one observes a sharp "phase lapse," where the maxima jump from even to odd multiples of π, due to an exact vanishing of the conductance which results from the Fano interference between the two resonances. These "lapses" are no longer sharp when $x \neq 0$: In the range $1 < \phi/\pi < 2$ there appears a relatively fast change of the maximum from around $\phi=2\pi$ down to $\phi \approx \pi$, similar to form B in Fig. 4. However, as ϕ increases

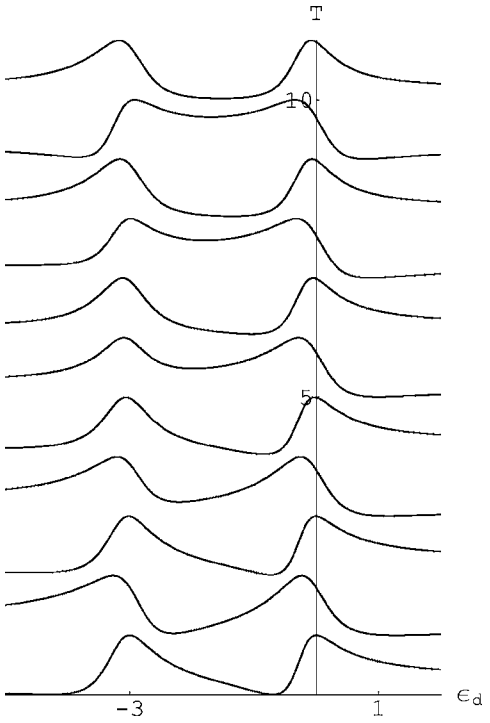

FIG. 8. Transmission through the ABI of Fig. 5, vs gate voltage ϵ_d, at $\phi=m\pi$. The graphs shift up by 1 as ϕ increases.

this lapse becomes smoother, and near $\phi=7\pi$ one no longer sees such a lapse at all, as in form A in Fig. 4. At fluxes of order π/x, the interplay between the two phases $\phi(1)$ and $\phi(2)$ destroys the exact vanishing of the transmission between resonances, and thus also destroys the phase lapses.

The interplay between the two fluxes also affects the dependence of the transmission on the gate voltage at fixed magnetic flux. Figure 8 shows this dependence for ϕ equal to integer multiples of π. Although qualitatively similar, the curves are not periodic in ϕ, and one can see variations of the Fano asymmetric shapes of the resonances with increasing flux.

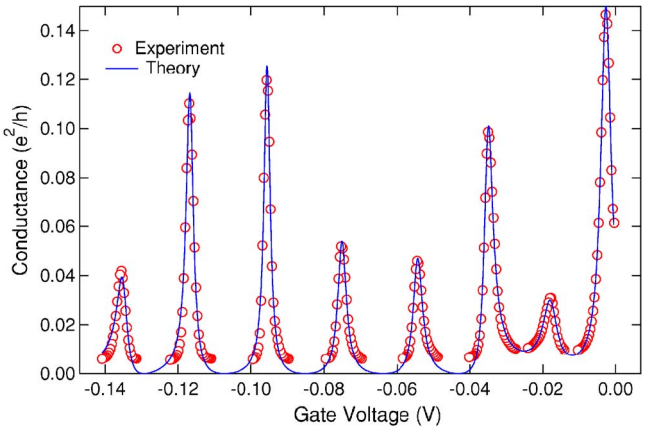

FIG. 9. (Color online) Conductance from the pinched off ABI. Red (circles): Experiment. Blue (full line): Fit to theory (see text).

Similar graphs also arise when one considers larger numbers of resonances. As long as one has $\phi(n)=[1+x(n)]\phi$, with $|x(n)|\ll 1$, the overall shapes of the graphs are found to be similar to those presented above. Apparently, in the vicinity of a specific resonance the results are mainly affected by neighboring resonances, so that only a small number of different fluxes participate in the "beats."

Before proceeding to fits of real data, we comment on the assumptions of our theoretical model. As stated, our aim is not to present a full description of the specific system, but rather to construct the *simplest* theoretical model which captures the relevant physics. Future work can include the following extensions: (i) One can shift the Fermi energy of the electrons, ϵ, away from the band center of the leads, $\epsilon=0$. In real experiments, the leads are not really one dimensional, and the Fermi energy is usually far away from the edges of the energy band, so that one does not expect a strong dependence of the results on ϵ. Indeed, Eq. (2) shows that a shift in ϵ can be replaced by a shift of all the other energies in our model [i.e., $E_D(n)$, E_{ref}]. In addition, for ka near $\pi/2$ the overall conductance in Eq. (3) has a relatively slow variation with ka, which becomes negligible near resonances. (ii) One

TABLE I. The parameters of our fits to Eq. (3). The conductance G is also assumed to have a background, $a+bV_g$, and the zero of V_g for the ABI is shifted by c relative to that of the pinched off case.

n	$J_\ell^0(n)/\sqrt{eJ}$ ($\times 10^{-2}$V$^{1/2}$)	$J_r(n)/\sqrt{eJ}$ ($\times 10^{-2}$V$^{1/2}$)	$(E_D(n)-\epsilon_d)/e$ (V)	$x(n)$ ($\times 10^{-2}$)
1	0.5886	3.860	0.0008	0
2	−3.761	0.3806	−0.0159	−5.913
3	3.708	0.4211	−0.0350	−0.069
4	3.876	0.2988	−0.0543	−0.085
5	3.716	0.3073	−0.0752	5.669
6	3.161	0.4030	−0.0956	−0.058
7	3.420	0.4155	−0.1168	−0.006
8	4.170	0.2934	−0.1353	0.069

ϕ_1 (rad)	a (e^2/h)	b (e^2/hV)	c (V)	$j_l/\sqrt{JE_{ref}}$	$j_r/\sqrt{JE_{ref}}$
1639.13	0.5392	0.7391	−0.01768	0.4224	0.1003

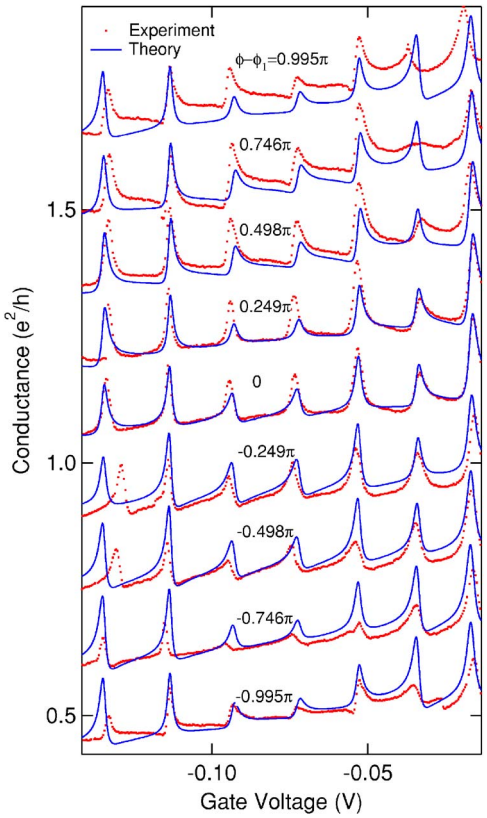

FIG. 10. (Color online) Conductance from the ABI. Red (dots): Experiment. Blue (full lines): Fit to theory (see text). Curves correspond to fields B between 0.9100 and 0.9132 T, each graph is shifted $0.15e^2/h$

can replace each branch in Fig. 5 (e.g., the bond between L and the n's resonance on the dot) by a tight binding chain, representing some internal structure. In practice, such a structure will only renormalize the effective hopping matrix element through such a chain.[19] We absorb any such structure into our parameters $J_x(n)$ and j_x. (iii) One can allow the quantum dot to have some internal structure, which might end up with some flux dependence of the corresponding eigenenergies $E_D(n)$. However, the small area of the dot would imply that the corresponding flux dependence only shows up at much higher fluxes, which are irrelevant for the experimentally interesting range. (iv) One can also replace the reference branch by a more complex structure. In practice, this branch only enters via the last term in Eq. (2), which could be replaced by a constant. Again, a modified structure would only renormalize this constant, thus requiring a different set of parameters in our fits. (v) Finally, one can allow for more internal structure to the ABI branches, e.g., replacing each branch by a lattice with a finite width.[10] Again, the small loops of such a lattice will only affect the results at very high fluxes. For the specific fits presented below, our simple model already requires many parameters (four parameters per resonance, plus the reference arm). Adding any of the above changes might add many more parameters, and probably improve the fits. However, as we show below, our minimal model already represents the data very well.

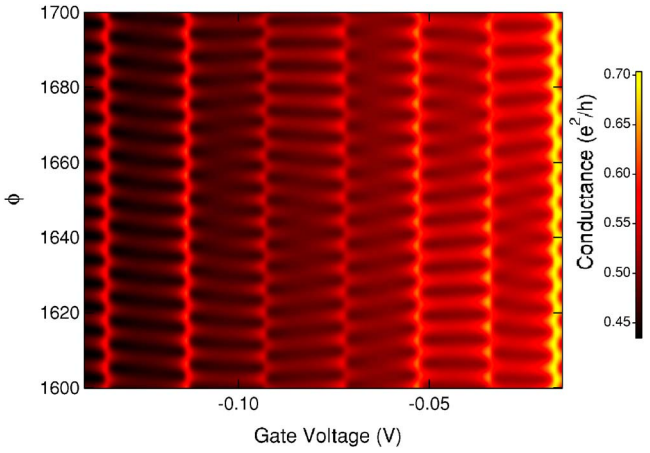

FIG. 11. (Color online) Calculated color scale plot of the conductance, using the parameters from Table I.

IV. FITS TO EXPERIMENTAL DATA

Equation (3) should represent a good approximation for any sequence of Coulomb blockade peaks, with and without a magnetic flux. Indeed, in Ref. 17 this equation has been applied to produce a reasonable imitation of the data found by Göres *et al.*[21] for a mesoscopic single electron transistor. The Fano asymmetry parameter for each resonance is in fact determined by the influence of all the other resonances and, therefore, there is no need for individual fits of q for each resonance and each set of parameters.

To demonstrate the effectiveness of Eq. (3), we have fitted it to data from Ref. 2 and to similar new data, which exhibit a sequence of Coulomb blockade resonances of the ABI, at various values of the magnetic flux. Here we chose a sequence of measurements, done on the device shown in Fig. 1 for gate voltages between −0.142 and −0.014 V and magnetic fields in the range 0.9100–0.9132 T. Figures 9 and 10 show fits to our data, using Eq. (3). As explained in Ref. 2, our device allows the pinch off of the reference path. Fitting Eq. (3) with $j_\ell = j_r = 0$ to the pinched off data, we have determined $E_D(n)$, $J_\ell^0(n)$, and $J_r(n)$, with $\phi(n)=0$. The results of this fit are shown in Fig. 9. Clearly, the fit is excellent. We have then added the reference path, and used the data from the ABI to determine $j_\ell/\sqrt{E_{ref}}$, $j_r/\sqrt{E_{ref}}$ (As discussed above, we use $\epsilon=0$, to represent electrons at the Fermi level, deep inside the band.) and the phases $\phi(n) \equiv [1+x(n)]\phi_1$ for one particular value of the magnetic field, $B_1=0.9116$ T. The results of this fit appear as the fifth graph from the bottom in Fig. 10. Repeating this fit for $B_2=0.9100$ T (the bottom curve in Fig. 10), using the same parameters except for replacing ϕ_1 by a fitted ϕ_2, we then found the coefficient C in the relation $\phi=\phi_1+C(B-B_1)$, $C=976.9\mathrm{T}^{-1}$.[22] In addition, our fit allows a background conductance which contains a component linear in the gate voltage, in addition to a constant. The resulting parameters are listed in Table I. Using these parameters, we have then produced the theoretical curves for all the other values of B, with no further adjustments (Fig. 10). The fits clearly capture all the qualitative changes in the shapes of the resonances at different magnetic fluxes. We find the results quite satisfactory, confirming the

assumptions of our theoretical model. We note that the fitted parameters have practically equidistant resonances, with $U \approx 0.02$ V. This Coulomb energy is consistent with the capacitance and area of the quantum dot.

Having obtained the parameters in Table I, we have then plotted the theoretical contour plot of the conductance, see Fig. 11. Qualitatively, this figure is similar to Fig. 4 (taken at a slightly different range of parameters): The maxima move continuously with the magnetic flux and with the gate voltage, imitating typical experimental data.

V. CONCLUSION

In this paper we have concentrated on the periodic effects of having a closed ABI with a ring which has a finite width. For a semiconductor ring, we argue that each resonance on the quantum dot can be associated with a single magnetic flux, which penetrates the wave function in the ring which couples to that resonance. A simple theoretical formula then captures all the qualitative features observed in many experiments. Adding more ingredients into the model would only add more parameters, potentially improving the (already excellent) fits.

ACKNOWLEDGMENTS

We acknowledge very helpful discussions with Y. Imry, and support from the Israel Science Foundation, under Grant No. 1566/04, and from a Grant-in-Aid for Scientific Research by the Japanese Ministry of Education, Science, Sports and Culture. A.A. and O.E.W. are also grateful to the ISSP for the warm hospitality.

*Email address: kats@issp.u-tokyo.ac.jp
†Present address: Toshiba Corporation, Research and Development Center, 1, Komukai Toshibacho, Saiwai-ku, Kawasaki-shi, 212-8582 Kanagawa, Japan.
‡Present address: Institute of Chemical Research, Kyoto University, Gokasho Uji, Kyoto 611-0011, Japan.

[1] A. Yacoby, M. Heiblum, D. Mahalu, and H. Shtrikman, Phys. Rev. Lett. **74**, 4047 (1995).
[2] K. Kobayashi, H. Aikawa, S. Katsumoto, and Y. Iye, Phys. Rev. Lett. **88**, 256806 (2002); J. Phys. Soc. Jpn. **71**, 2094 (2002); Phys. Rev. B **68**, 235304 (2003).
[3] S. Datta, M. R. Melloch, S. Bandyopadhyay, R. Noren, M. Vaziri, M. Miller, and R. Reifenberger, Phys. Rev. Lett. **55**, 2344 (1985); G. Cernicchiaro, T. Martin, K. Hasselbach, D. Mailly, and A. Benoit, *ibid.* **79**, 273 (1997); S. Pedersen, A. E. Hansen, A. Kristensen, C. B. Sørensen, and P. E. Lindelof, Phys. Rev. B **61**, 5457 (2000).
[4] A. Yacoby, R. Schuster, and M. Heiblum, Phys. Rev. B **53**, 9583 (1996).
[5] For a review, see G. Hackenbroich, Phys. Rep. **343**, 463 (2001).
[6] L. Onsager, Phys. Rev. **38**, 2265 (1931); H. B. G. Casimir, Rev. Mod. Phys. **17**, 343 (1945); M. Büttiker, Phys. Rev. Lett. **57**, 1761 (1986).
[7] Y. Gefen, Y. Imry, and M. Ya. Azbel, Phys. Rev. Lett. **52**, 129 (1984); A. L. Yeyati and M. Büttiker, Phys. Rev. B **52**, R14360 (1995); A. Aharony, O. Entin-Wohlman, and Y. Imry, Phys. Rev. Lett. **90**, 156802 (2003); see also the review in Ref. 5.
[8] G. Hackenbroich and H. A. Weidenmüller, Phys. Rev. Lett. **76**, 110 (1996).
[9] R. A. Webb, S. Washburn, C. P. Umbach, and R. B. Laibowitz, Phys. Rev. Lett. **54**, 2696 (1985).
[10] A. D. Stone, Phys. Rev. Lett. **54**, 2692 (1985).
[11] A. D. Stone and Y. Imry, Phys. Rev. Lett. **56**, 189 (1986).
[12] Y. Imry, *Introduction to Mesoscopic Physics*, 2nd ed. (Oxford University Press, Oxford, 2002), p. 119.
[13] U. F. Keyser, C. Fühner, S. Borck, R. J. Haug, M. Bichler, G. Abstreiter, and W. Wegscheider, Phys. Rev. Lett. **90**, 196601 (2003).
[14] M. Sigrist, A. Fuhrer, T. Ihn, K. Ensslin, S. E. Ulloa, W. Wegscheider, and M. Bichler, Phys. Rev. Lett. **93**, 066802 (2004).
[15] U. Fano, Phys. Rev. **124**, 1866 (1961).
[16] O. Entin-Wohlman, A. Aharony, Y. Imry, and Y. Levinson, J. Low Temp. Phys. **126**, 1251 (2002).
[17] A. Aharony, O. Entin-Wohlman, and Y. Imry, Turk. J. Phys. **27**, 299 (2003).
[18] We neglect here the magnetic width of the wave functions, which may be important at much high fields.
[19] A. Aharony, O. Entin-Wohlman, B. I. Halperin, and Y. Imry, Phys. Rev. B **66**, 115311 (2002).
[20] R. Landauer, Philos. Mag. **21**, 863 (1970).
[21] J. Göres, D. Goldhaber-Gordon, S. Heemeyer, M. A. Kastner, H. Shtrikman, D. Mahalu, and U. Meirav, Phys. Rev. B **62**, 2188 (2000).
[22] For the fits at $B=B_1$, each $x(n)$ is determined only up to the addition of $2\pi m(n)/\phi_1$, with integer $m(n)$. We have also added small shifts to the parameters of peaks 1 and 2 to compensate some instability in the dot.